



## Full Length Article

## Improved prediction of reaction kinetics for amine absorbent-based carbon capture using reactive site-based transition state conformer search method



Qilei Liu<sup>a</sup>, Sheng Xiang<sup>a</sup>, Jian Du<sup>a</sup>, Qingwei Meng<sup>a,b</sup>, Jianbing Chen<sup>c</sup>, Ming Gao<sup>c</sup>, Bing Xing<sup>c</sup>, Lei Zhang<sup>a,\*</sup>

<sup>a</sup> State Key Laboratory of Fine Chemicals, Frontiers Science Center for Smart Materials Oriented Chemical Engineering, Institute of Chemical Process Systems Engineering, School of Chemical Engineering, Dalian University of Technology, Dalian 116024, China

<sup>b</sup> Ningbo Research Institute, Dalian University of Technology, Ningbo 315016, China

<sup>c</sup> SINOPEC (Dalian) Research Institute of Petroleum and Petrochemicals Co., Ltd, Dalian 116045, China

## ARTICLE INFO

## Keywords:

Carbon capture  
Amine absorbent  
Reaction kinetics  
Transition state  
Conformational isomer

## ABSTRACT

There is no doubt that carbon emissions are one of the greatest challenges facing humanity today. Carbon capture, utilization, and storage is an effective way to achieve carbon neutrality. However, the commonly used commercial absorbents for post-combustion captures still have some limitations such as low chemical absorption rate constants. In this paper, a universal reaction kinetic model is developed for amine-based carbon capture based on the transition state theory, density functional theory, and hybrid solvation model. The developed reaction kinetic model is applicable to a wide range of amine-solvent solutions involving primary/secondary/tertiary amines and aqueous/nonaqueous solvents. The key contribution of this work is developing a reactive site-based search method for the GENeration of Conformers for Transition States (GENConf-TS). GENConf-TS has greatly improved the prediction accuracy of the reaction kinetic model from  $R^2 = 0.882$  to  $R^2 = 0.950$  based on a dataset of 23 various amine-solvent solutions. The results highlight the critical impacts of the transition state conformational isomers on amine-based CO<sub>2</sub> chemical absorption rate constants.

## 1. Introduction

The increasing development of human society, economy and industry has resulted in a growing demand for fossil fuels in various production activities. As a result of burning fossil fuels, a significant amount of greenhouse gases are produced, causing a series of environmental problems, including global warming and extreme weather conditions. According to the sixth assessment report of the Intergovernmental Panel on Climate Change (IPCC), the average annual global greenhouse gas emissions from 2010 to 2019 were at the highest level in human history, but the growth rate has slowed down. However, the goal of limiting global warming to around 2 °C still requires a peak in global greenhouse gas emissions by 2025 at the latest, as well as a quarter decrease in emissions by 2030 [1]. As the main gas causing the greenhouse effect, the absorption and disposal of carbon dioxide (CO<sub>2</sub>) has always been an issue of widespread concern. Carbon Capture, Utilization and Storage (CCUS) is widely deemed as a key technology to reduce CO<sub>2</sub> emissions from large industrial facilities. According to the IPCC report, modern conventional power plants equipped with CCUS

technology can reduce CO<sub>2</sub> emissions to the atmosphere by 80–90 % [2]. There is no doubt that CCUS has the potential to reduce CO<sub>2</sub> emissions in the short term, but the high cost and energy requirements of current CO<sub>2</sub> capture methods make it a challenging technological option [3]. Generally, the carbon capture technology can be divided into the pre-combustion capture, oxy-fuel combustion capture, and post-combustion capture [4]. In general, the post-combustion capture is considered the most feasible method of capturing CO<sub>2</sub> as it has a mature technology and is easy to integrate with other industrial processes. There are a number of common methods for post-combustion capture, including the membrane separation [5,6], physical adsorption [7,8], and chemical absorption [9,10]. Although the membrane separation method has developed rapidly, it still has its own limitations due to CO<sub>2</sub> partial pressure in the feed gases and achieving high capture efficiencies via membranes is a big challenge. Thus, the membrane separation method is not widely used in industry. The limitation of physical adsorptions is that the amount of absorption is usually not large enough. Chemical absorption first appeared in the 1930s and is widely used in industrial CO<sub>2</sub> capture owing to its advantages of large absorption capacity

\* Corresponding author.

E-mail address: [keleiz@dlut.edu.cn](mailto:keleiz@dlut.edu.cn) (L. Zhang).

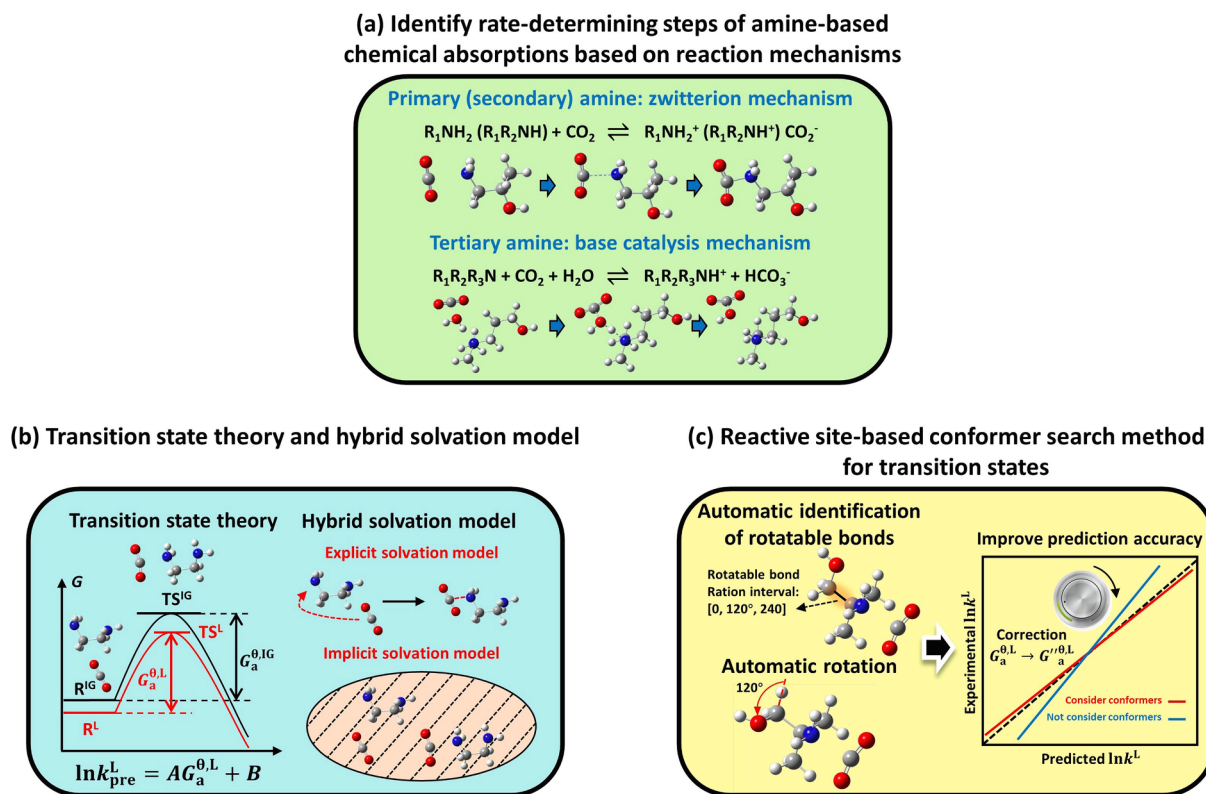


**Fig. 1.** An overview of the development procedure of the universal reaction kinetic model for amine-based carbon capture and the relationship between the kinetic model and the reactive site-based transition state conformer search method.

and fast absorption rate. One of the most important factors in chemical absorptions is the choice of  $CO_2$  absorption medium [11,12].

There are a number of commonly used absorbents, including the aqueous ammonia [13], potassium carbonate [14], ionic liquid [15], amine [16], and so on. Aqueous ammonia absorbents have large absorption capacities and low energy consumptions for regeneration, but their reaction rate is slow and they are highly volatile, making them prone to cause secondary pollution [17]. Potassium carbonates are low in cost and highly stable, but their absorption rates are slow and often require the addition of expensive catalysts [18]. Ionic liquids have low vapor pressure and sound thermal stability, however, they have several disadvantages, including the complicated and costly synthesis steps, high viscosity and a large mass transfer resistance that reduces the heat transfer coefficient [19]. Compared with other absorbents, amines have the advantages of large absorption capacity, rapid absorption rate, and low operating costs [20,21]. Amine compounds have been widely studied in  $CO_2$  capture. The representative absorbents are monoethanolamine (MEA) [22], diethanolamine (DEA) [23], and methyl-diethanolamine (MDEA) [24]. However, these amines still have certain limitations. For example, MEA and DEA are primary and secondary amines with limited  $CO_2$  loadings, respectively. In addition, a high level of energy is required for amine regeneration due to the high stability of the carbamate produced by chemical absorptions. Although the tertiary amine MDEA has a large  $CO_2$  loading and a low regeneration energy, its chemical absorption rate is slow [25]. In order to address the shortcomings of current amines and explore amines with good performance in  $CO_2$  loading, regeneration energy, and chemical absorption rate, numerous researchers have studied the influence of amine structures on their performances through experiments and modeling methods. For example, Liu et al. [26] investigate the steric hindrance effect on the reaction rate constants of chemical reactions between  $CO_2$  and amines that include MEA and its four different substituent products. Singh et al. [27] study the effects of chain length, side chain, number of functional

groups (amine groups) and other factors on  $CO_2$  absorption rates.

Although a number of experiments have been conducted in order to investigate the absorption properties of amines with different structures extensively in the last few decades, yet a significant number of potential high-performance molecules remain undiscovered. Compared with the experimental approach, the first principle-based molecular simulation methods (e.g., Density Functional Theory (DFT), Hartree-Fock, etc.) provide a relatively cost-effective means for screening or designing molecules with desired properties. DFT has been widely used to study the reaction kinetics of  $CO_2$  absorption by amines [28]. For example, Silva et al. [29] employ the DFT method to study the chemical reactions between  $CO_2$  and amine systems, and analyze the important factors affecting the overall reactivity. Xie et al. [30] use the DFT method to calculate activation energies for the reactions between a series of substituted monoethanolamines and  $CO_2$ , and investigate the effect of substituents on reaction kinetics. On the basis of the experimental work of Chowdhury et al. [31], Rozanska et al. [32] study the absorption properties of 24 types of tertiary amine aqueous solutions through the DFT method and the molecular dynamics simulation, establishing a quantitatively accurate model for predictions of absorption rate constants. Nevertheless, their model has not considered primary/secondary amines and other nonaqueous solvents, which hinders the application of their model to explore more potential amines. Although the DFT method has been widely used by scholars to study the reactions between amines and  $CO_2$ , there is still no universal reaction kinetic mechanism model that is highly accurate and widely applicable. One of the largest challenges is that the conformational effect of transition states and reactants has a significant effect on reaction kinetics, but few efficient and automatic conformer search methods are available for transition states.

To this end, an efficient and automatic reactive site-based conformer search method for transition states is developed in this work. It is used to develop a universal reaction kinetic mechanism model based on the transition state theory and the DFT method for accurate predictions of

$\text{CO}_2$  chemical absorption rate constants in various amine-solvent solutions involving primary, secondary, tertiary amines and water, methanol, ethanol solvents. By utilizing the transition state conformer search method, the prediction accuracy of the reaction kinetic model is significantly enhanced. Given a novel amine structure, the developed accurate reaction kinetic model is able to predict its amine-based  $\text{CO}_2$  chemical absorption rate constants without any experimental data. This paper is organized as follows. In the second section, the developments of the reaction kinetic model and the conformer search method for transition states are introduced. In the third section, the prediction results of the reaction kinetic model with/without the conformer search method are presented and discussed. Also, the influence mechanism of the transition state conformers on reaction kinetics of amine-based  $\text{CO}_2$  chemical absorptions are studied by the analysis methods of weak interactions and reactive site charges.

## 2. Reaction kinetic model for amine-based carbon capture considering transition state conformers

In this section, a universal reaction kinetic model is developed for amine-based carbon capture, where a reactive site-based search method for the GENeration of Conformers for Transition States (GENConf-TS) is proposed to enhance the model prediction accuracy. An overview of the development procedure of the reaction kinetic model and the relationship between the kinetic model and the transition state conformer search method is presented in Fig. 1.

In the first step (Fig. 1(a)), the rate-determining reaction steps of amine-based  $\text{CO}_2$  chemical absorptions are first identified based on the reaction mechanisms. Then, in the second step (Fig. 1(b)), a reaction kinetic model is formulated by correlating chemical absorption rate constants (i.e., reaction rate constant in amine-solvent solutions  $k^L$ ) with activation Gibbs free energies at liquid state based on the transition state theory and the hybrid solvation model. The model parameters are fitted with the DFT calculated activation energies and the experimental  $k^L$  through the least square method. With the model parameters,  $k^L$  is able to be successfully predicted once the information of amine-solvent solutions is input to the reaction kinetic model. In the third step (Fig. 1(c)), a reactive site-based conformer search method for transition states is developed to further improve the prediction accuracy of the reaction kinetic model. The developed reaction kinetic model in this work involves all chemical absorption mechanisms for primary, secondary, and tertiary amines, as well as includes both aqueous and nonaqueous solvents. In the following subsections, the reaction kinetic mechanisms for amine absorptions, the transition state theory and hybrid solvation model used in the reaction kinetic model, as well as the conformer search method for transition states are presented in detail. Note that a simplification has been made that only the monoamine systems are considered in this work. The more complex mixed amine systems will be considered in our future work.

### 2.1. Identify rate-determining steps of amine-based chemical absorptions based on reaction mechanisms

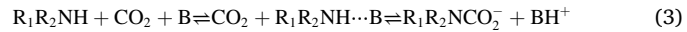
Amine refers to the product in which one or more hydrogen atoms in the ammonia molecule are replaced by hydrocarbon groups. According to the number of hydrogen atoms replaced in the amine molecule, amines can be divided into primary, secondary, and tertiary amines. The reaction mechanisms of amine-based  $\text{CO}_2$  absorptions can be divided into three categories according to literatures.

The first category is the zwitterionic mechanism for primary and secondary amines [33], which includes two steps: the first step is the formation of an intermediate zwitterion (Eq. (1)), and the second step is the deprotonation of the zwitterion by reacting with a base (Eq. (2)). In these steps,  $\text{R}_1\text{R}_2\text{NH}$  represents a primary amine or a secondary amine if  $\text{R}_2$  is a hydrogen atom or  $\text{R}_1$  and  $\text{R}_2$  are neither hydrogen atoms, respectively. The symbol B represents an amine, water, hydroxide or

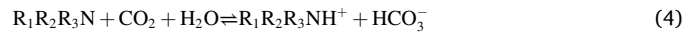
other substances that is used as a base.



The second category is the trimolecular reaction mechanism for primary and secondary amines [34]. In this mechanism, the reaction between an amine and  $\text{CO}_2$  forms an unstable complex rather than a zwitterion, and the complex is then regenerated into a carbamate through the direct reaction among an amine,  $\text{CO}_2$ , and a base molecule (Eq. (3)).



The third category is the base catalysis mechanism for tertiary amines [35], believing that the tertiary amine does not react directly with  $\text{CO}_2$  like the primary and secondary amines as there is no H atom on the N atom in the tertiary amine. The mechanism holds the opinion that tertiary amines will form hydrogen bonds with water to increase the reactivity of  $\text{CO}_2$  and water (Eq. (4)).



According to literatures [36,37], researchers have compared the reaction energy barriers of two mechanisms (Eq. (1) and Eq. (3)) for amine-aqueous solvent (water) solutions through the DFT methods. The results show that the reaction energy barriers of the zwitterion mechanism (Eq. (1)) are lower than those of the trimolecular reaction mechanism (Eq. (3)), indicating that the zwitterionic mechanism is more suitable to describe the  $\text{CO}_2$  chemical absorptions in amine-aqueous solvent (water) solutions. Besides, the literatures find that the rate of the second reaction step in the zwitterion mechanism is generally faster than that of the first step. Thus, the first reaction step in the zwitterionic mechanism is usually the rate-determining step. Furthermore, it is found that only the amine reacts with  $\text{CO}_2$  in the first reaction step, indicating that the use of nonaqueous solvents (alcohols) should not alter the first reaction step of the zwitterion mechanism. Therefore, this work uses the first reaction step of the zwitterion mechanism (Eq. (1)) as the rate-determining reaction step to study the primary and secondary amine-based  $\text{CO}_2$  chemical absorptions for both aqueous and nonaqueous solvents. As for tertiary amines, the rate-determining reaction step (Eq. (4)) in the base catalysis mechanism is considered.

### 2.2. Transition state theory and hybrid solvation model

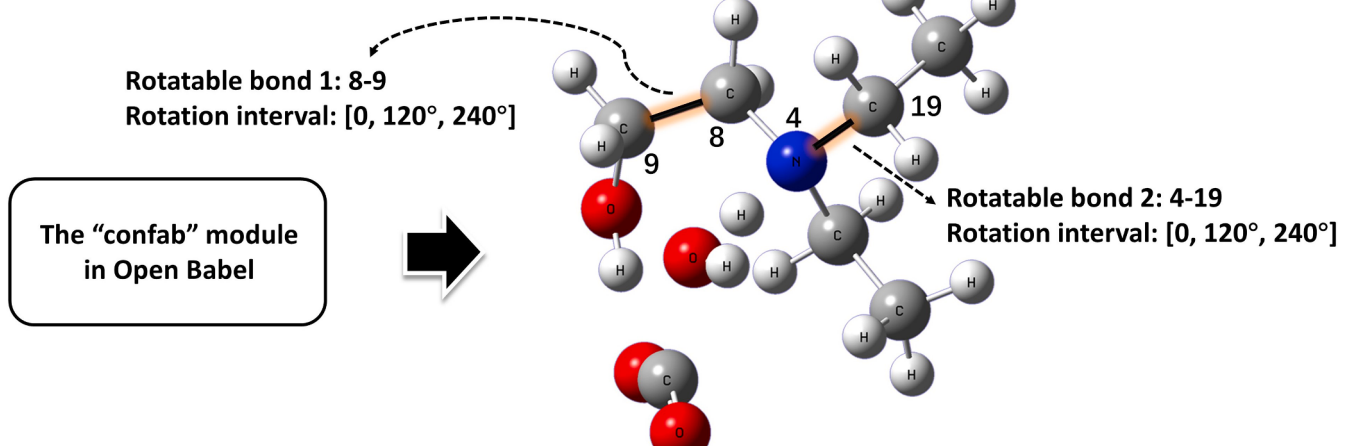
Based on the analyses of the amine-based chemical absorption mechanisms, the next step is to develop a universal reaction kinetic model for predictions of  $\text{CO}_2$  chemical absorption rate constants. The kinetic model can be primarily formulated by the transition state theory, as shown in Eqs. (5–6).

$$k^{0,L} = \kappa \frac{k_B T}{h} \prod_i (\text{c}_i^{0,L})^{\nu_i} \exp\left(-\frac{G_a^{0,L}}{RT}\right), i = \text{TS, R} \quad (5)$$

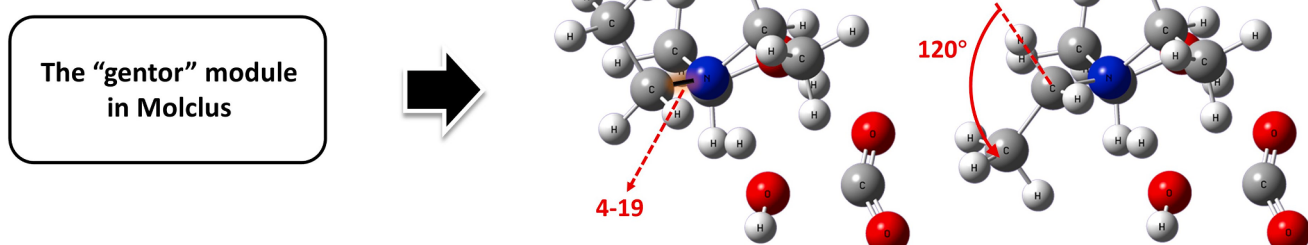
$$G_a^{0,L} = \sum_i \nu_i G_i^{0,L} = \sum_i \nu_i (G_i^{0,IG} + \Delta G_i^{0,p \rightarrow c} + \Delta G_i^{0,solv}), i = \text{TS, R} \quad (6)$$

where  $k^{0,L}$  is the standard reaction rate constant in liquid phase,  $\kappa$  is the dimensionless transmission coefficient (assume to be a constant in this work),  $k_B$  is the Boltzmann constant,  $T$  is the reaction temperature,  $h$  is the Planck constant,  $\text{c}_i^{0,L}$  is the liquid phase standard state concentration of compound  $i$  ( $\text{c}_i^{0,L} = 1 \text{ mol/L}$ ),  $\nu_i$  is the stoichiometric coefficient of compound  $i$ ,  $G_a^{0,L}$  is the standard activation Gibbs free energy in liquid phase,  $R$  is the universal gas constant, TS represents the transition state, R represents the reactants.  $G_i^{0,IG}$  denotes the standard Gibbs free energies of compound  $i$  in gas phase, which is predicted by the DFT method.  $\Delta G_i^{0,p \rightarrow c}$  is the Gibbs free energy change of compound  $i$  from a pressure-

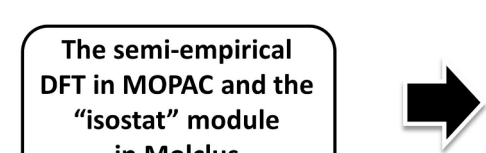
### (a) Automatically identify rotatable bonds



### (b) Automatically rotate bonds



### (c) Automatically cluster conformers



Isomer	Boltzmann distribution	Enthalpy of formation (a.u.)
1	24.00%	-0.400178
2	19.36%	-0.399976
3	8.83%	-0.399234
4	8.22%	-0.399166
.....		

Fig. 2. The schematic diagram of the reactive site-based conformer search method for transition states.

based standard state at 1 atm to a concentration-based standard state at 1 mol/L for an ideal gas ( $\Delta G_i^{\theta,p \rightarrow c} = 7.91 \text{ kJ/mol}$  at 298.15 K and 1 atm).  $\Delta G_i^{\theta,\text{solv}}$  is the standard solvation free energy of compound  $i$ .

Then, two adjustable parameters ( $C_1$  and  $C_2$ ) are added to Eq. (5) to correct the reaction kinetic model by minimizing the prediction errors between the predicted  $k^L$  ( $k_{\text{pre}}^L$ ) and the experimental  $k^L$  ( $k_{\text{exp}}^L$ ), as shown in Eq. (7). Once the temperature and pressure are determined, Eq. (7) can be converted to Eq. (8).

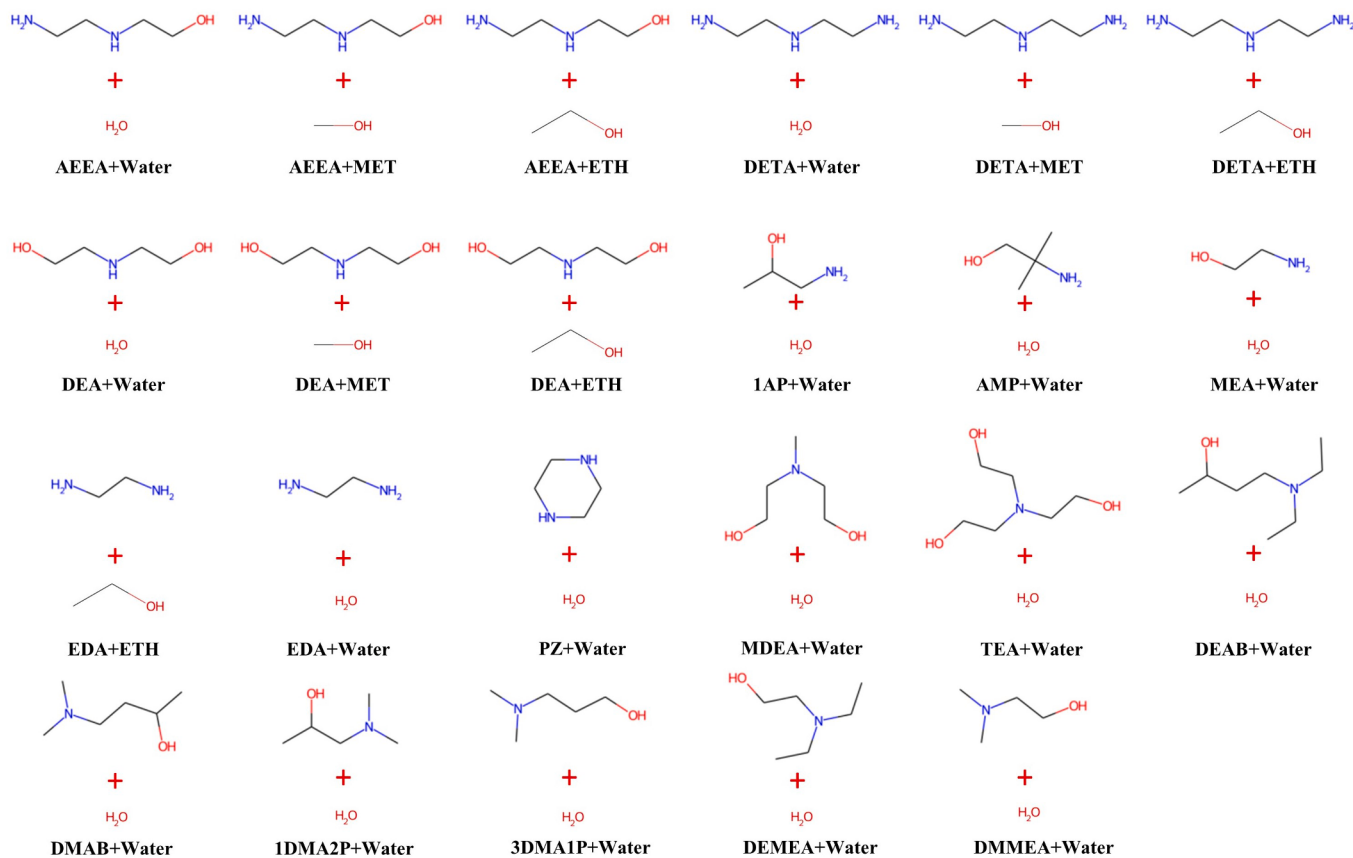
$$k_{\text{pre}}^L = C_1 \kappa \frac{k_B T}{h} \prod_i (c_i^{\theta,L})^{\nu_i} \exp\left(-\frac{C_2 G_a^{\theta,L}}{RT}\right), i = \text{TS, R} \quad (7)$$

$$\ln k_{\text{pre}}^L = AG_a^{\theta,L} + B = A \sum_i \nu_i G_i^{\theta,L} + B \\ = A \sum_i \nu_i (G_i^{\theta,\text{IG}} + \Delta G_i^{\theta,p \rightarrow c} + \Delta G_i^{\theta,\text{solv}}) + B, i = \text{TS, R} \quad (8)$$

where the new adjustable parameter  $A$  equals to  $-C_2/RT$ , and another new parameter  $B$  equals to  $\ln(C_1 \kappa k_B T \prod_i (c_i^{\theta,L})^{\nu_i} / h)$ . These two parameters are fitted with the  $k_{\text{exp}}^L$  and the DFT calculated  $G_a^{\theta,L}$  through the least

square method. Therefore,  $G_i^{\theta,\text{IG}}$  and  $\Delta G_i^{\theta,\text{solv}}$  are two key physical quantities that need to be calculated by the DFT method.

Considering that amine-solvent solutions play the roles of reactants and reaction solvents in chemical absorption systems, it is necessary to employ the hybrid solvation model to describe transition states in solvent environments. The hybrid solvation model is composed of the explicit and implicit solvation models. The explicit solvation model is carried out to determine the three-dimensional spatial relationship among amine, solvent and  $\text{CO}_2$  by searching the transition states of rate-determining reactions. The implicit solvation model is used to simulate solvent environments during the transition state search process. The tasks of the transition state search and the frequency analysis for transition states are performed to obtain the thermal correction to standard Gibbs free energy  $G_{\text{TS}}^{\theta,\text{corr}}$  through the DFT calculations with the method of B3LYP functional, the basis set of 6-31G(d), the dispersion correction based on the Becke-Johnson (BJ) damping function, and the implicit solvation model (Solvation Model based on Density (SMD) [38]) in Gaussian 09 software [39]. Afterwards, the task of single point energy calculation is performed for the transition state to obtain total electronic energy  $E_{\text{TS}}$  with the method of M062x functional, the basis set of def2tzvp, the dispersion correction based on the zero damping function.



**AEEA:** N-(2-Hydroxyethyl)ethylenediamine; **DETA:** Diethylenetriamine; **DEA:** Diethanolamine; **1AP:** 1-Aminopropan-2-ol; **AMP:** Aminomethylpropanol; **MEA:** Monoethanolamine; **EDA:** Ethylenediamine; **PZ:** Piperazine; **MDEA:** Methyl diethanolamine; **TEA:** Triethanolamine; **DEAB:** 4-(Diethylamino)butan-2-ol; **DMAB:** 4-(Dimethylamino)butan-2-ol; **1DMA2P:** 1-Dimethylamino-2-propanol; **3DMA1P:** 3-Dimethylamino-1-propanol; **DEMEA:** Diethylethanolamine; **DMMEA:** Dimethylethanolamine; **MET:** Methanol; **ETH:** Ethanol.

Fig. 3. The amine-solvent solutions studied in this work.

$G_{TS}^{0,IG}$  is then calculated through  $G_{TS}^{0,IG} = G_{TS}^{0,corr} + E_{TS}$ . Next, the SMD model is carried out to obtain  $\Delta G_{TS}^{0,solv}$ , where the method of M052x functional and the basis set of 6-31G(d) are adopted in this step. Similar DFT tasks are performed for the reactants of amine, solvent, and CO<sub>2</sub> using the same DFT level.

### 2.3. Reactive site-based conformer search method for transition states

A molecule may have different conformational isomers with distinct Gibbs free energies due to the hydrogen-bonding effect, conjugation effect, and so on. Since a large number of N—H and O—H bonds in amine-solvent-CO<sub>2</sub> systems will form intermolecular hydrogen bonds and affect the reaction energy barriers [40], it is necessary to consider the influences of conformational effects of reactants and transition states on  $G_a^{0,L}$ .

The automatic conformer search method for reactants is available in known software, including Open Babel [41], Molclus [42], and so on. However, to our best knowledge, the known conformer search methods are hard to be directly applied to transition states as they are either generally worked to identify the minimum points rather than the saddle points along the potential energy surface [41] or need to set rotatable bonds manually [42]. Therefore, it is desirable to develop an efficient and automatic conformer search method for transition states to find the most stable transition state with the lowest energy among its conformers for each rate-determining reaction. To this end, an efficient and

automatic reactive site-based conformer search method for transition states is developed in this work. Its working principle is to freeze the reactive sites of transition states first, and then rotate the side chains that link to the reactive sites to find potential conformational isomers for transition states.

More specifically, the transition state conformer search method is carried out through three steps, as shown in Fig. 2. In the first step (Fig. 2(a)), the “confab” module in the Open Babel [41] software is employed to automatically identify the rotatable bonds and the rotation intervals for transition states. In this work, two modifications are made to the obtained rotatable bonds to avoid the Cartesian coordinate variations of the reactive sites. First, if two atoms linked by a certain rotatable bond both belong to the reactive sites, this rotatable bond is deleted. Second, the atomic numbers of the atoms close to the reactive sites need to be written on the left side of the rotatable bond string. For example, in Fig. 2(a), the rotatable bond string “9–8” is given by the Open Babel software and it needs to be modified to “8–9”. This is because the side chain attached to the atom on the right side of the rotatable bond string is set to be rotated in the next step. In the second step (Fig. 2(b)), the “gentor” module in the Molclus software [42] is employed to automatically generate a large number of “pseudo” conformational isomers through rotating the rotatable bonds according to the rotation intervals ergodically. In the third step (Fig. 2(c)), the semi-empirical DFT method (e.g., PM7) in the MOPAC software [43] is used to optimize the generated “pseudo” conformational isomers. During this process, the reactive

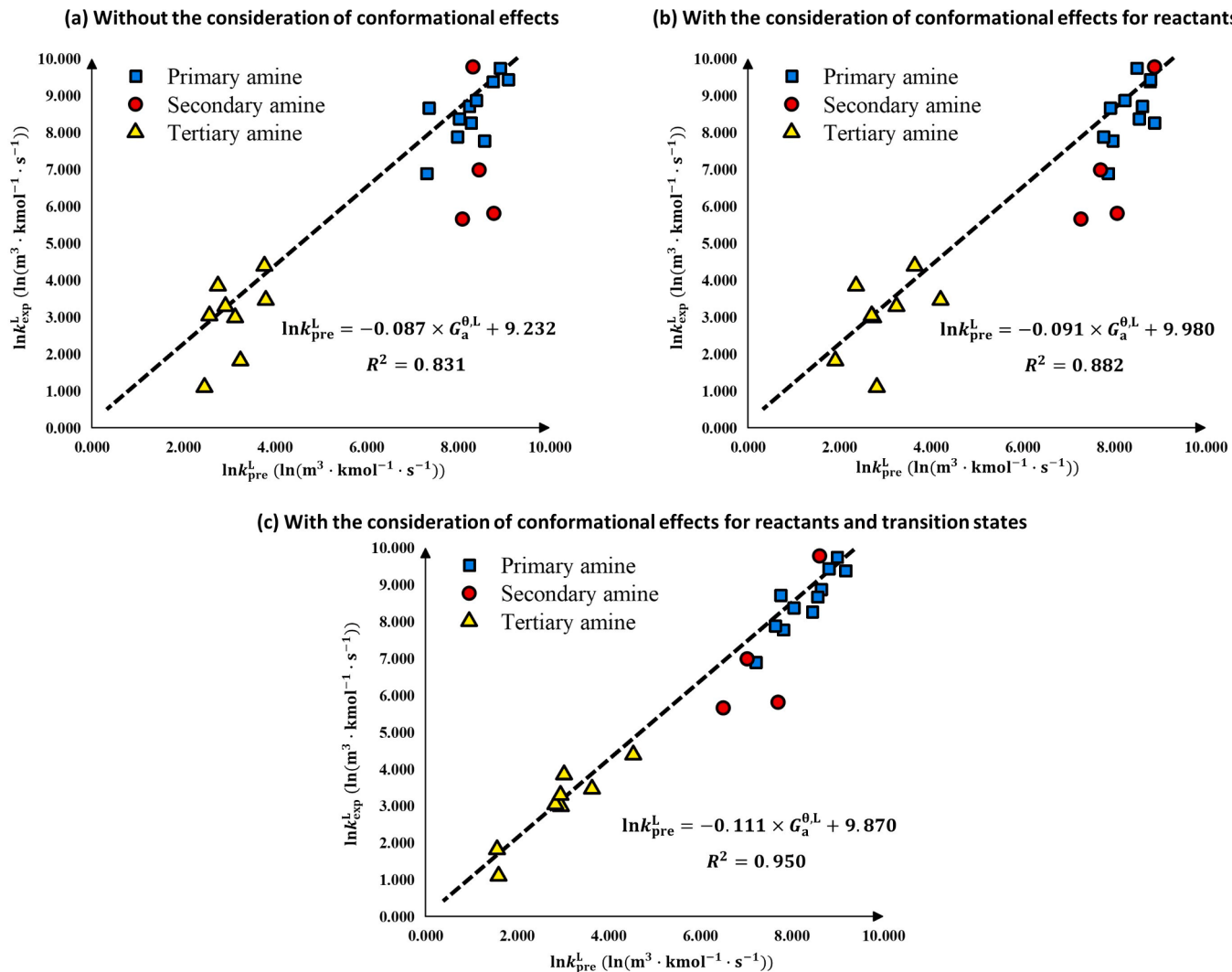


Fig. 4. The regression results of the reaction kinetic models.

sites are frozen. The optimized results are then processed with the “isostat” module in the Molclus software [42] to cluster similar conformational isomers of transition states. The obtained conformational isomers are finally ranked according to their standard enthalpies of formation and the Boltzmann distribution at a certain temperature. Note that the reliability of ranking conformers depends on the energy calculation methods to some extent. It is suggested to select a certain number of top ranked conformers rather than only the top ranked one for further rigorous evaluations if the energy calculation methods are not rigorous.

After using the known conformer search method for reactants and the developed reactive site-based conformer search method for transition states, a few top ranked conformers of reactants and transition states are respectively selected for further rigorous DFT calculations in this work. The corrected activation Gibbs free energies,  $G_a^{\theta,L}$  and  $G_a^{\theta,TS}$ , are calculated based on only the reactant conformer with the lowest  $G_R^{\theta,L}$ , as well as based on both the reactant and transition state conformers with the lowest  $G_R^{\theta,L}$  and  $G_{TS}^{\theta,L}$ , respectively. Finally, the reaction kinetic model considering the conformational effect is developed by fitting the model parameters ( $A$  and  $B$  in Eq. (8)) with  $G_a^{\theta,L}$  ( $G_a^{\theta,TS}$ ) and  $k_{\text{exp}}^L$ . However, our conformer search approach has two shortcomings. One is that it fails to search the conformers of alicyclic rings. According to the principle of our conformer search method, if the rotatable bonds in the alicyclic rings are identified and rotated, some covalent bonds in the

alicyclic ring will be destroyed. The other one is that it cannot handle on the molecule with too many rotatable bonds (usually more than eight), as there will be a combinatorial explosion in sampling space. These shortcomings will be addressed by integrating our method with the simulated annealing approach based on molecular dynamics in the future work.

### 3. Results and discussions

#### 3.1. Performance of reaction kinetic model for amine-based carbon capture

In this work, a total number of 23 different amine-solvent solutions with corresponding  $k_{\text{exp}}^L$  are used to develop a universal reaction kinetic model for predictions of amine-based CO<sub>2</sub> absorption rate constants, as shown in Fig. 3. Ten top ranked reactants and transition states obtained by the known conformer search method for reactants and the developed reactive site-based conformer search method for transition states are selected for each reaction system. The  $G_a^{\theta,L}$ ,  $G_a^{\theta,TS}$ , and  $G_a^{\theta,TS}$  of each reaction system are calculated through the DFT method without the consideration of conformational effects for only reactants, and with the consideration of conformational effects for both reactants and transition states, respectively. The obtained  $G_a^{\theta,L}/G_a^{\theta,TS}/G_a^{\theta,TS}$  are linearly fitted with  $k_{\text{exp}}^L$  through

**Table 1**

The values of DFT calculated activation Gibbs free energies and experimental reaction rate constants for each amine-solvent solution.

Amine-solvent solution	$G_a^{\theta,L}$ (kJ/mol) <sup>a</sup>	$G_a'^{\theta,L}$ (kJ/mol) <sup>b</sup>	$G_a''^{\theta,L}$ (kJ/mol) <sup>c</sup>	$\ln k_{\exp}^L(\ln(m^3 \cdot kmol^{-1} \cdot s^{-1}))$
AAEA-H <sub>2</sub> O	7.322	13.823	6.278	9.401 [44]
AAEA-MET	9.487	22.742	14.721	7.800 [45]
AAEA-ETH	16.244	24.981	13.714	7.908 [45]
DETA-H <sub>2</sub> O	5.567	16.992	7.926	9.770 [46]
DETA-MET	13.234	15.666	8.748	8.734 [45]
DETA-ETH	11.528	19.901	10.240	8.892 [45]
DEA-H <sub>2</sub> O	10.620	25.512	25.512	7.003 [47]
DEA-MET	6.931	21.526	19.427	5.823 [23]
DEA-ETH	14.787	30.219	30.219	5.670 [47]
1AP-H <sub>2</sub> O	15.745	16.473	16.473	8.396 [48]
AMP-H <sub>2</sub> O	23.889	23.889	23.889	6.914 [49]
MEA-H <sub>2</sub> O	23.342	23.344	11.766	8.690 [50]
EDA-H <sub>2</sub> O	3.535	13.767	9.545	9.457 [51]
EDA-ETH	12.791	12.791	12.791	8.284 [45]
PZ-H <sub>2</sub> O	12.152	12.565	11.222	9.800 [52]
MDEA-H <sub>2</sub> O	70.235	89.135	74.804	1.819 [53]
TEA-H <sub>2</sub> O	79.193	79.193	74.500	1.099 [54]
DEAB-H <sub>2</sub> O	75.834	84.177	61.600	3.855 [55]
DMAB-H <sub>2</sub> O	71.544	80.075	62.203	2.993 [55]
1DMA2P-H <sub>2</sub> O	77.972	80.423	63.319	3.044 [54]
3DMA1P-H <sub>2</sub> O	63.885	63.886	56.086	3.466 [54]
DEMEA-H <sub>2</sub> O	64.223	70.097	47.950	4.394 [54]
DMMEA-H <sub>2</sub> O	73.948	74.481	62.300	3.296 [56]

**Eq. (8).** Note that the reaction temperatures for all reaction systems are 298.15 K. Fig. 4 shows the regression results of reaction kinetic models. Table 1 gives the specific values of  $G_a^{\theta,L}$ ,  $G_a'^{\theta,L}$ ,  $G_a''^{\theta,L}$  and  $\ln k_{\exp}^L$  for each reaction system. As shown in Fig. 4, the data points of primary/secondary amine-based reaction systems are basically distributed on the right side, while the data points of tertiary amine-based reaction systems are distributed on the left side. If the conformational effect is not considered for reactants and transition states (Fig. 4(a)), the distribution of each data point is relatively scattered, and the determination coefficient ( $R^2$ ) of the model regression results is 0.831. If the conformer search methods are used for only reactants and both reactants and transition states, the  $R^2$  of the reaction kinetic model has significantly improved from 0.831 to 0.882 and 0.831 to 0.950, respectively, indicating the necessity of considering the conformational isomer issue in developing reaction kinetic models and demonstrating the feasibility and effectiveness of our transition state conformer search method in further enhancing the prediction accuracy of the reaction kinetic model. The results are consistent with the fact that the closer the transition

states and reactants are to their reality states (i.e., the lowest energy state), the more accurate the reaction kinetic model behaves.

### 3.2. Influence mechanism of transition state conformational isomers on activation Gibbs free energies

In this subsection, two analysis methods involving weak interactions and reactive site charges are carried out for the transition state conformers to provide insights into the influence mechanism of transition state conformers on activation Gibbs free energies. For the convenience of illustrating the energy differences between conformers in a reaction system, a baseline energy is set for one conformer at 0 kJ/mol, and the relative energies of the other two conformers are then calculated based on the baseline value. Here, the Independent Gradient Model based on Hirshfeld partition (IGMH) [57] method is utilized to make intuitive descriptions of the weak interactions. Besides, the Atomic Dipole moment Corrected Hirshfeld (ADCH) [58] method is used to determine the atomic charges of reactive sites in conformers, which is calculated using the Multiwfn [59] software and visualized by the VMD [60] software.

MEA-H<sub>2</sub>O (primary amine), a widely used commercial amine-solvent solution, is first taken as an example, along with its three typical conformers of transition states (Fig. 5). The IGMH results for the transition state conformers in the MEA-H<sub>2</sub>O system is shown in Fig. 6. The ADCH charge differences between the reactive sites of the C atom in CO<sub>2</sub> and the N atom in amine (2C-7N), as well as the relative activation Gibbs free energies of the transition state conformers in the MEA-H<sub>2</sub>O system, are given in Table 2. From Figs. 5 and 6, it can be observed that only the interaction force between the two atoms located at the reaction sites (2C-7N) exists in this amine-solvent system. Table 2 reveals that the conformer (Fig. 5(c)) exhibits a larger ADCH charge difference compared with the other two conformers (Fig. 5(a) and 5(b)). This implies that the reactants, CO<sub>2</sub> and amine, are more likely to react with each other through the minimum energy path involving the transition state conformer (Fig. 5(c)). Additionally, the obtained ADCH results conform to the qualitative ranking of relative activation Gibbs free energies.

DEA-H<sub>2</sub>O (secondary amine), as a typical secondary amine-solvent solution, is then taken as an example, along with its three typical conformers of transition states (Fig. 7). The IGMH results for the transition state conformers in the DEA-H<sub>2</sub>O system is shown in Fig. 8. The ADCH charge differences between the reactive sites of the C atom in CO<sub>2</sub> and the N atom in amine (8C-1N), as well as the relative activation Gibbs free energies of the transition state conformers in the DEA-H<sub>2</sub>O system, are given in Table 3. From Figs. 7 and 8, it is seen that the O atom in CO<sub>2</sub> has a weak interaction (hydrogen-bonding interaction) with the H atom in amine among three conformers. This hydrogen-bonding interaction is beneficial to the attractions between 8C-1N reactive sites, the

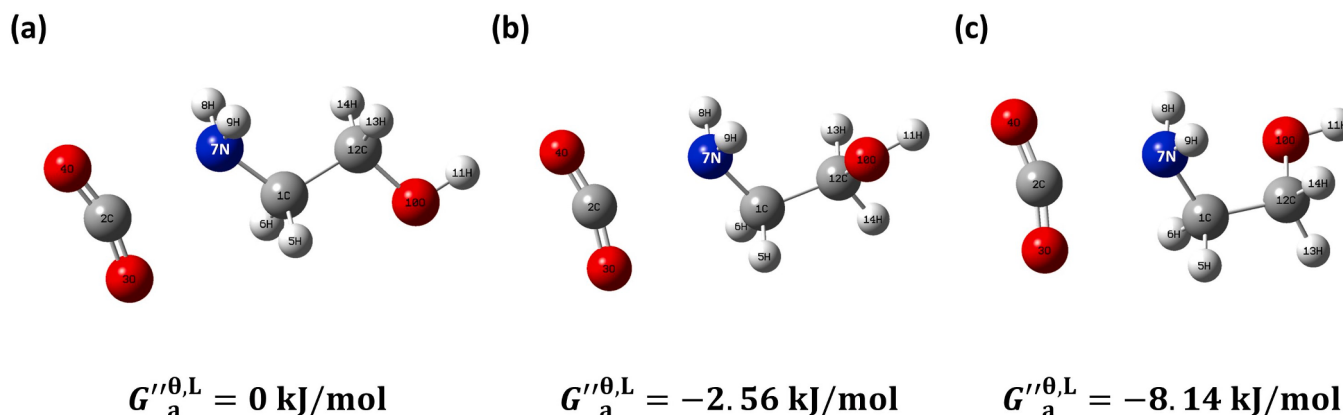


Fig. 5. Three typical conformers of transition states in the MEA-H<sub>2</sub>O system.

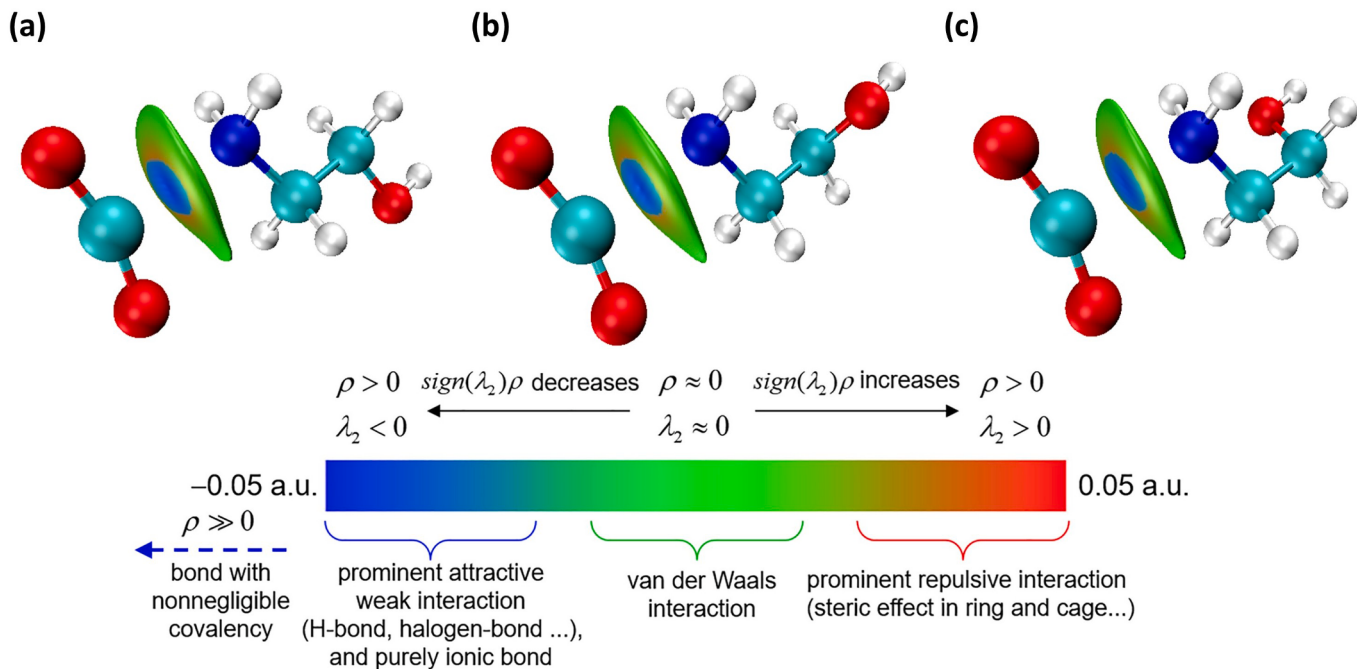


Fig. 6. The IGMH results for the transition state conformers in the MEA-H<sub>2</sub>O system.

Table 2

The ADCH charge differences between the reactive sites of the C atom in CO<sub>2</sub> and the N atom in amine (2C-7N), as well as the relative activation Gibbs free energies of the transition state conformers in the MEA-H<sub>2</sub>O system.

Conformer	ADCH charge difference of 2C-7N (a.u.)	$G''^{\theta,\text{L}}_{\text{a}}$ (kJ/mol)
(a)	0.6442	0
(b)	0.6466	-2.56
(c)	0.6491	-8.14

interaction of which is also identified in Fig. 8. From Table 3 it is found that the ADCH charge difference of 8C-1N in the conformer (Fig. 7(b)) is larger than those of the other two conformers (Fig. 7(a) and 7(c)), indicating that the reactants of CO<sub>2</sub> and amine are easier to react with each other through the minimum energy path that involves the transition state conformer (Fig. 7(b)). This result is also consistent with the qualitative ranking of relative activation Gibbs free energies, which confirms the validity of the calculated results regarding activation Gibbs free energies to some extent. The ADCH charge differences among

reactive sites could provide an explanation for the variations in energy caused by conformational changes.

MDEA-H<sub>2</sub>O (tertiary amine), another commonly used amine-solvent solution, is also taken as an example, along with its three typical conformers of transition states (Fig. 9). The IGMH results for the transition state conformers in the MDEA-H<sub>2</sub>O system is shown in Fig. 10. Note that there are two pairs of reactive sites in the MDEA-H<sub>2</sub>O system as it follows the base catalysis mechanism of tertiary amines. Therefore, the ADCH charge differences between the C atom in CO<sub>2</sub> and the O atom in water (1C-5O), those between the N atom in amine and the H atom in water (7N-4H), as well as the summation of the 1C-5O and 7N-4H charge differences are considered in this example. The ADCH charge differences, as well as the relative activation Gibbs free energies of the transition state conformers in the MDEA-H<sub>2</sub>O system, are given in Table 4. As shown in Fig. 9, the O atom in CO<sub>2</sub> tends to form a hydrogen-bonding interaction with the H atom on the hydroxyl group in amine. Compared with the conformers (Fig. 9(a) and 9(b)) that only have one hydrogen bond, there are two more hydrogen bonds in the conformer (Fig. 9(c)), including one interaction between the O atom in hydroxyl group and the

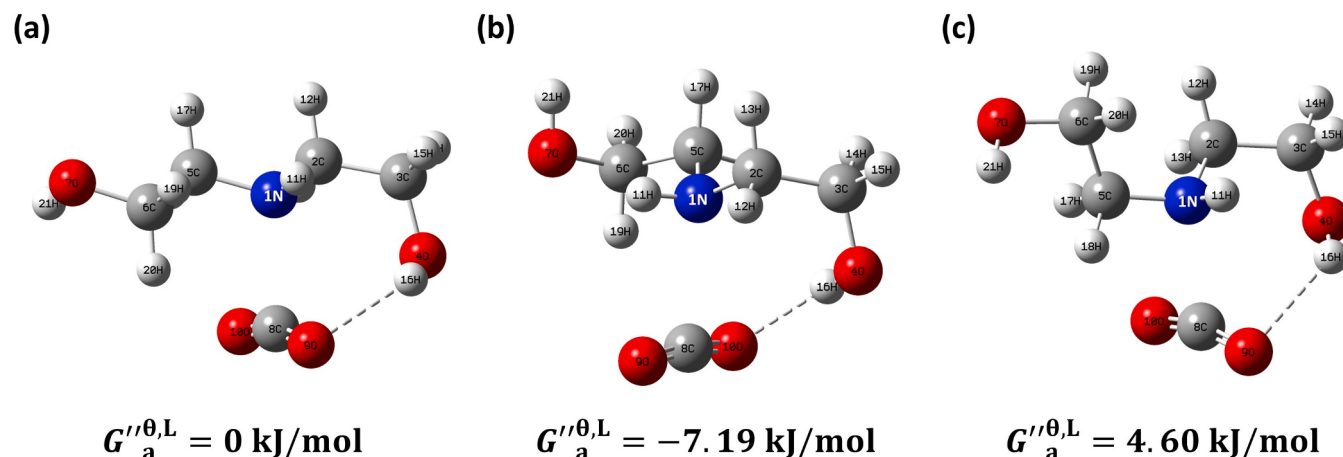


Fig. 7. Three typical conformers of transition states in the DEA-H<sub>2</sub>O system.

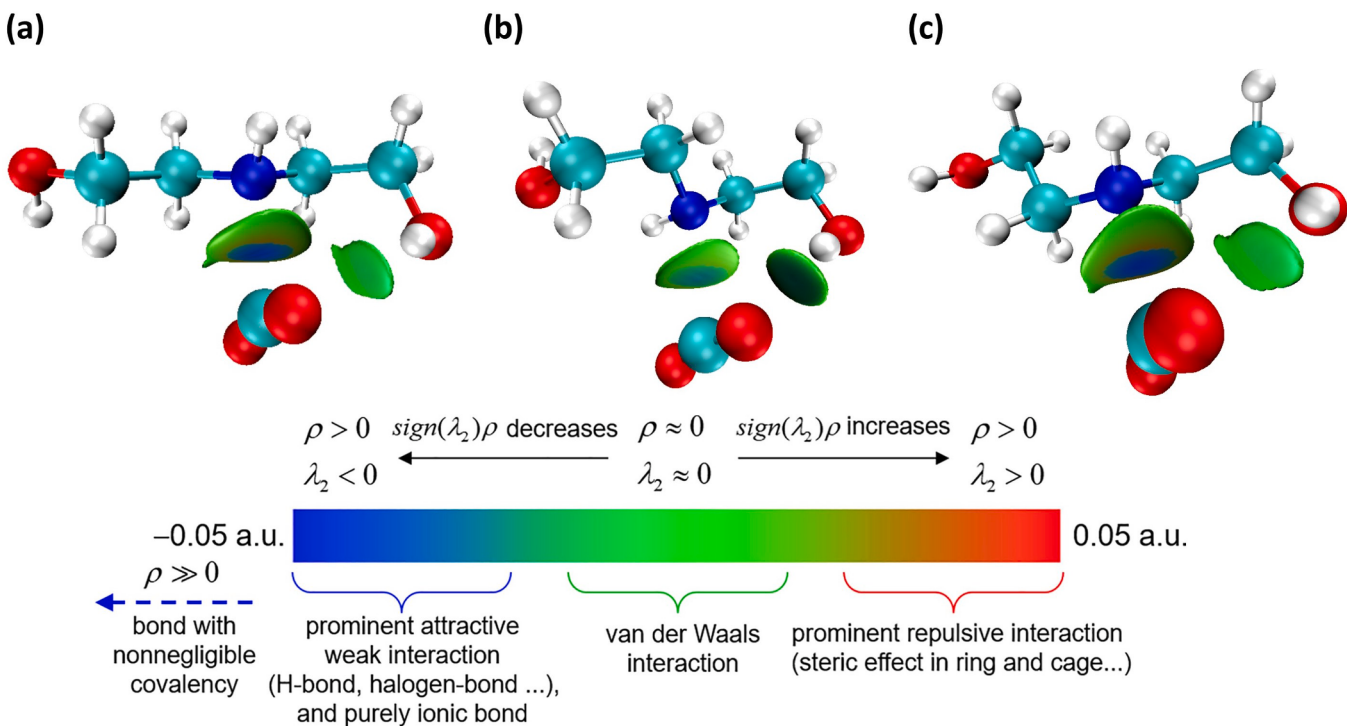
Fig. 8. The IGMH results for the transition state conformers in the DEA-H<sub>2</sub>O system.

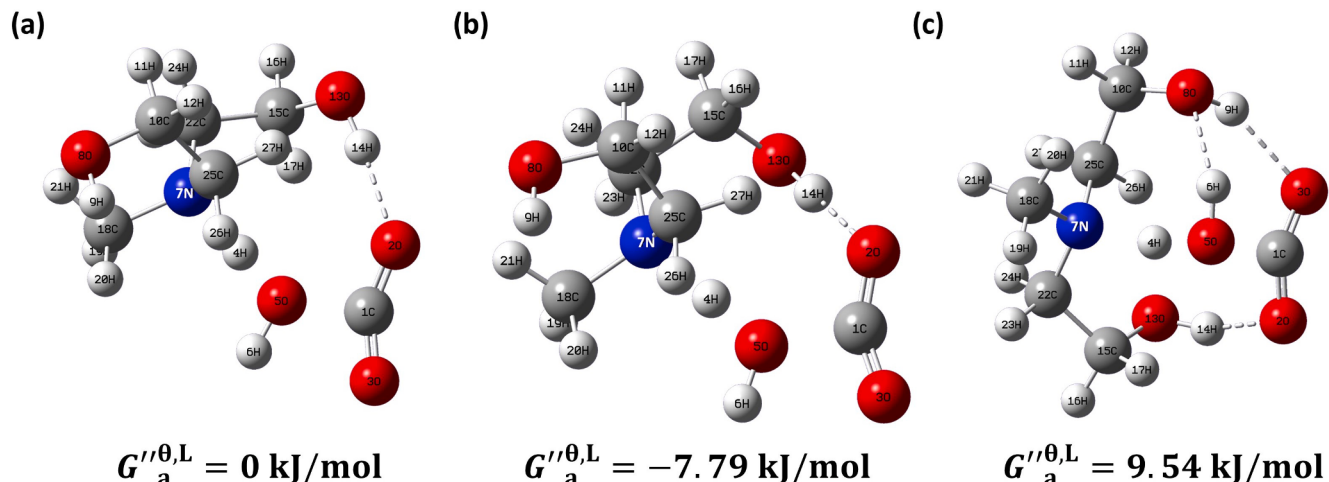
Table 3

The ADCH charge differences between the reactive sites of the C atom in CO<sub>2</sub> and the N atom in amine (8C-1N), as well as the relative activation Gibbs free energies of the transition state conformers in the DEA-H<sub>2</sub>O system.

Conformer	ADCH charge difference of 8C-1N (a.u.)	$G_a^{\theta, L}$ (kJ/mol)
(a)	0.5284	0
(b)	0.6348	-7.19
(c)	0.4469	4.60

H atom in water (8O-6H), and another interaction between the H atom in hydroxyl group and the O atom in CO<sub>2</sub> (14H-2O). Fig. 10 also identifies the interactions observed in Fig. 9 and the critical weak interactions among two pairs of reactive sites (1C-5O and 7N-4H). Although the number of hydrogen bonds in the conformer (Fig. 9(c)) is more than that in the conformers (Fig. 9(a) and 9(b)) and the hydrogen-

bonding interaction (8O-6H) is able to accelerate the reaction process by improving the 7N-4H attractions, the overall reaction process is still limited by the hydrogen-bonding interaction (14H-2O) according to the base catalysis mechanism of tertiary amines because the 14H-2O interaction cooperates with the hydrogen-bonding interaction (9H-3O) to hinder the attack of CO<sub>2</sub> to water. The above weak interaction analysis is able to explain why the activation Gibbs free energy of the conformer (Fig. 9(c)) is larger than those of the other two conformers (Fig. 9(a) and 9(b)). From Table 4 it is found that the summation of the ADCH charge differences of 7N-4H and 1C-5O in the conformer (Fig. 9(b)) is larger than those of the other two conformers (Fig. 9(a) and 9(c)), indicating that the reactants of CO<sub>2</sub> and amine are easier to react with each other through the minimum energy path that involves the transition state conformer (Fig. 9(b)). This result is also consistent with the qualitative ranking of relative activation Gibbs free energies, which confirms the validity of the calculated results regarding activation Gibbs free

Fig. 9. Three typical conformers of transition states in the MDEA-H<sub>2</sub>O system.

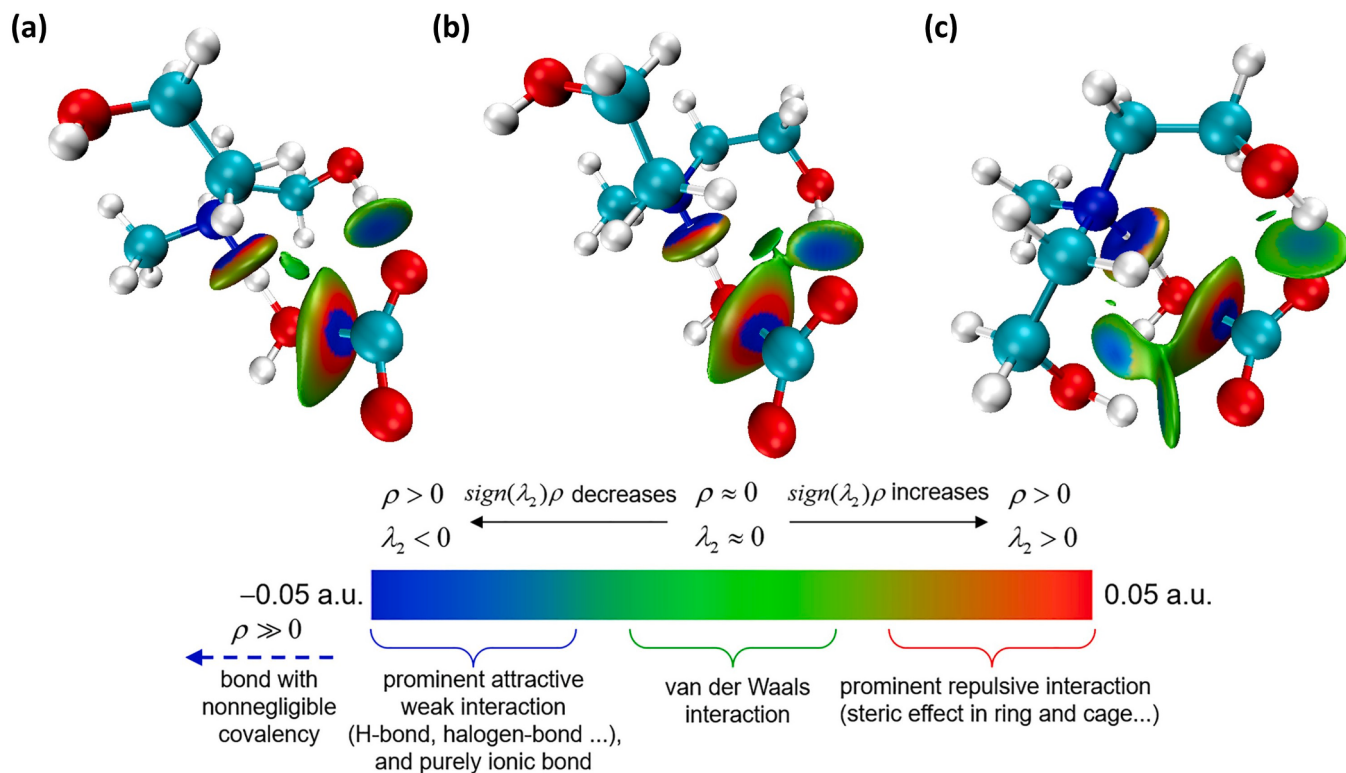


Fig. 10. The IGMH results for the transition state conformers in the MDEA-H<sub>2</sub>O system.

Table 4

The ADCH charge differences between the reactive sites of the C atom in CO<sub>2</sub> and the O atom in water (1C-5O), and those of the N atom in amine and the H atom in water (7N-4H), as well as the relative activation Gibbs free energies of the transition state conformers in the MDEA-H<sub>2</sub>O system.

Conformer	ADCH charge difference of 7N-4H (a.u.)	ADCH charge difference of 1C-5O (a.u.)	Total ADCH charge difference (a.u.)	$G_a^{\text{act,L}}$ (kJ/mol)
(a)	0.1591	0.7662	0.9253	0
(b)	0.1640	0.7712	0.9352	-7.79
(c)	0.1711	0.7535	0.9246	9.54

energies.

The analysis results of the MEA-H<sub>2</sub>O, DEA-H<sub>2</sub>O and MDEA-H<sub>2</sub>O systems highlight the necessity of considering the impacts of the transition state conformer variations on reactivities. The calculations of weak interactions and reactive site charges also demonstrate the rationality of ranking for transition state conformers based upon activation Gibbs free energies predicted by the conformer search method and DFT calculations.

### 3.3. Heuristic rules involving amine substituents

The variation of amine substituents often has a great impact on amine-based CO<sub>2</sub> absorption rate constants. For example, Jorgensen et al. [61] report that using the electron-donating amine substituents (e.g., NH<sub>2</sub>CH<sub>3</sub>, etc.) or increasing the number of substituents on amines is able to improve the interaction between CO<sub>2</sub> and amine. Xiao et al. [62] study ten commercial tertiary amines and find that the ethyl group and the side carbon chain are able to promote the activity of tertiary amine, and the increase of hydroxyl group is able to reduce the reaction rate. The study by Muchan et al. [63] shows that the increase in the number of amine groups is able to increase the absorption rate of CO<sub>2</sub>. This work

Table 5

The relationship between the numbers of functional groups and the values of experimental reaction rate constants.

Amine-solvent system	Hydroxyl group	Amine group	$\ln k_{\text{exp}}^L (\ln (\text{m}^3 \cdot \text{kmol}^{-1} \cdot \text{s}^{-1}))$
DETA-H <sub>2</sub> O	0	2	9.770
AEEA-H <sub>2</sub> O	1	1	9.401
DEA-H <sub>2</sub> O	2	0	7.003

also finds that the  $k_{\text{exp}}^L$  of three structurally similar amines (DETA, AEEA, and DEA) increase with the decrease of their numbers of hydroxyl groups and the increase of their numbers of amine groups, as shown in Table 5.

Here, some heuristic rules involving amine substituents are summarized as follows. These rules can be served as the structure constraints for the optimization-based mathematical programming model [64], which is able to design amines-based CO<sub>2</sub> absorbents in a high-throughput manner.

- (1) The amine-based CO<sub>2</sub> absorption rates increase if the hydroxyl group in amines is replaced by the amine group. The amine group is an electron-donating group, which is able to enhance the electric charge density of the N atom in reactive sites of amines.
- (2) The amine-based CO<sub>2</sub> absorption rates increase if the hydroxyl group is far away from the N atom in reactive sites of amines. Hydroxyl group is an electron-accepting group, which is capable of decreasing the electric charge density of the N atom in reactive sites of amines (e.g., 3DMA1P and 1DMA2P).

## 4. Conclusion

Reaction kinetics is a key evaluation criterion for amine-based carbon capture process. A universal reaction kinetic mechanism model is developed in this paper for predictions of reaction rate constants for CO<sub>2</sub>

chemical absorptions based on the transition state theory, the DFT method, and the hybrid solvation model. The developed reaction kinetic model covers a wide range of 23 reaction systems involving primary/secondary/tertiary amines and aqueous/nonaqueous solvents. The key contribution of this work is proposing a reactive site-based conformational isomer search method for transition states (GENConf-TS). The proposed GENConf-TS method has significantly enhanced the prediction accuracy of the universal reaction kinetic model from  $R^2 = 0.882$  to  $R^2 = 0.950$ , demonstrating its successful application in modeling the reaction kinetics of amine-based CO<sub>2</sub> chemical absorptions. Compared with the semi-empirical and empirical modeling methods, our mechanism model only needs two adjustable parameters regressed by the experimental data, and has a strong interpretability for CO<sub>2</sub> absorption process. Two analysis methods of IGMH and ADCH involving weak interactions and reactive site charges, respectively, are also carried out to provide insights into the influence mechanism of transition state conformational isomers on activation Gibbs free energies. The analysis results verify the rationality of ranking transition state conformers by activation energies, confirming the effectiveness of our conformational isomer search method in searching for stable transition state conformers with high existing probability.

Despite the sound performance of our reaction kinetic model for predicting CO<sub>2</sub> absorption rate constants, other absorption properties, including absorption capacity, absorption solubility, desorption energy consumption, have not been considered in this paper. An optimization-based mathematical programming model consisting of the reaction kinetic model developed in this work, the property constraints of other absorption properties, and the heuristic rule-based structure constraints will be studied in our future research.

#### CRediT authorship contribution statement

**Qilei Liu:** Conceptualization, Data curation, Formal analysis, Funding acquisition, Methodology, Project administration, Resources, Software, Supervision, Validation, Writing – review & editing. **Sheng Xiang:** Conceptualization, Data curation, Formal analysis, Investigation, Methodology, Software, Validation, Visualization, Writing – original draft. **Jian Du:** Project administration, Resources, Supervision. **Qingwei Meng:** Project administration, Resources, Supervision. **Jianbing Chen:** Project administration, Resources. **Ming Gao:** Project administration, Resources. **Bing Xing:** Project administration, Resources. **Lei Zhang:** Funding acquisition, Project administration, Resources, Supervision, Writing – review & editing.

#### Declaration of competing interest

The authors declare that they have no known competing financial interests or personal relationships that could have appeared to influence the work reported in this paper.

#### Data availability

The data has been shared in the article.

#### Acknowledgement

The authors are grateful for the financial supports of National Natural Science Foundation of China (22208042, 22078041, 22278053), China Postdoctoral Science Foundation (2022M710578), and “the Fundamental Research Funds for the Central Universities” (DUT22YG218).

#### References

- [1] IPCC, Climate change 2022: mitigation of climate change, in Cambridge: Cambridge University Press; 2022.
- [2] Metz B, et al. *IPCC special report on carbon dioxide capture and storage*. Cambridge: Cambridge University Press; 2005.
- [3] Zhao D, et al. Comprehensive analysis of thermodynamic models for CO<sub>2</sub> absorption into a blended N, N-diethylethanamine-1,6-hexamethyl diamine (DEEA-HMDA) amine. *AIChE J* 2023;69(10).
- [4] Rubin ES, et al. The outlook for improved carbon capture technology. *Prog Energy Combust Sci* 2012;38(5):630–71.
- [5] Feron P. Membranes for carbon dioxide recovery from power plants. In: *Carbon Dioxide Chemistry*. Elsevier; 1994. p. 236–49.
- [6] He XZ. A review of material development in the field of carbon capture and the application of membrane-based processes in power plants and energy-intensive industries. *Energy Sustain Society* 2018;8(34).
- [7] Ishibashi M, Otake K, Kanamori S. Study on CO<sub>2</sub> removal technology from flue gas of thermal power plant by physical adsorption method. *Greenhouse Gas Control Technol* 1999;95.
- [8] Builes S, et al. Microporous carbon adsorbents with high CO<sub>2</sub> capacities for industrial applications. *PCCP* 2011;13(35):16063–70.
- [9] Rochelle GT. Amine Scrubbing for CO<sub>2</sub> Capture. *Science* 2009;325(5948):1652–4.
- [10] Yang L, Chang C-W, Lin S-T. A novel multiscale approach for rapid prediction of phase behaviors with consideration of molecular conformations. *AIChE J* 2016;62(11):4047–54.
- [11] D’Alessandro DM, Smit B, Long JR. Carbon dioxide capture: Prospects for new materials. *Angew Chem Int Ed* 2010;49(35):6058–82.
- [12] Quan H, et al. Generic AI models for mass transfer coefficient prediction in amine-based CO<sub>2</sub> absorber, Part II: RBFNN and RF model. *AIChE J* 2023;69(1).
- [13] Yang N, et al. Aqueous ammonia (NH<sub>3</sub>) based post combustion CO<sub>2</sub> capture: a review. *Oil Gas Sci Technol-Revue D Ifp Energies Nouvelles* 2014;69(5):931–45.
- [14] Ayittey FK, et al. Parametric study and optimisation of hot K<sub>2</sub>CO<sub>3</sub>-based post-combustion CO<sub>2</sub> capture from a coal-fired power plant. *Greenhouse Gases-Sci Technol* 2020;10(3):631–42.
- [15] Yang QW, et al. New insights into CO<sub>2</sub> absorption mechanisms with amino-acid ionic liquids. *ChemSusChem* 2016;9(8):806–12.
- [16] Liu S, et al. Kinetics and new Bronsted correlations study of CO<sub>2</sub> absorption into primary and secondary alkanolamine with and without steric-hindrance. *Sep Purif Technol* 2020;233.
- [17] Fang M, et al. Experimental study on CO<sub>2</sub> absorption into aqueous ammonia-based blended absorbents. *Energy Procedia* 2014;61:2284–8.
- [18] Qi G, et al. Integrated bench-scale parametric study on CO<sub>2</sub> capture using a carbonic anhydrase promoted K<sub>2</sub>CO<sub>3</sub> solvent with low temperature vacuum stripping. *Ind Eng Chem Res* 2016;55(48):12452–9.
- [19] Ramdin M, de Loos TW, Vlugt TJH. State-of-the-art of CO<sub>2</sub> capture with ionic liquids. *Ind Eng Chem Res* 2012;51(24):8149–77.
- [20] Bai L, et al. Comprehensive technical analysis of CO<sub>2</sub> absorption into a promising blended amine of DEEA-HMDA. *Chem Eng Sci* 2023;280:119025.
- [21] Quan H, et al. Mass transfer mechanism and model of CO<sub>2</sub> absorption into a promising DEEA-HMDA solvent in a packed column. *Sep Purif Technol* 2023;320:124095.
- [22] Sema T, et al. *Mass transfer of CO<sub>2</sub> absorption in hybrid MEA-methanol solvents in packed column*. In: *International Conference on Greenhouse Gas Technologies (GHGT)*. 2012. Kyoto, JAPAN.
- [23] Park SW, et al. Reaction kinetics of carbon dioxide with diethanolamine in polar organic solvents. *Sep Sci Technol* 2005;40(9):1885–98.
- [24] Ermatchkov V, Pérez-Salado Kampas Á, Maurer G. Solubility of carbon dioxide in aqueous solutions of N-methylol diethanolamine in the low gas loading region. *Ind Eng Chem Res* 2006;45(17):6081–91.
- [25] Liu HL, et al. CO<sub>2</sub> absorption kinetics of 4-diethylamine-2-butanol solvent using stopped-flow technique. *Sep Purif Technol* 2014;136:81–7.
- [26] Liu B, et al. Reaction kinetics of the absorption of carbon dioxide (CO<sub>2</sub>) in aqueous solutions of sterically hindered secondary alkanolamines using the stopped-flow technique. *Chem Eng Sci* 2017;170:16–25.
- [27] Singh P, Versteeg GF. Structure and activity relationships for CO<sub>2</sub> regeneration from aqueous amine-based absorbents. *Process Saf Environ Prot* 2008;86(5):347–59.
- [28] Yang X, et al. Computational modeling and simulation of CO<sub>2</sub> capture by aqueous amines. *Chem Rev* 2017;117(14):9524–93.
- [29] da Silva EF, Svendsen HF. Computational chemistry study of reactions, equilibrium and kinetics of chemical CO<sub>2</sub> absorption. *Int J Greenhouse Gas Control* 2007;1(2):151–7.
- [30] Xie H, et al. Toward rational design of amines for CO<sub>2</sub> capture: Substituent effect on kinetic process for the reaction of monoethanolamine with CO<sub>2</sub>. *J Environ Sci* 2015;37:75–82.
- [31] Chowdhury FA, et al. CO<sub>2</sub> capture by tertiary amine absorbents: a performance comparison study. *Ind Eng Chem Res* 2013;52(24):8323–31.
- [32] Rozanska X, Wimmer E, de Meyer F. Quantitative kinetic model of CO<sub>2</sub> absorption in aqueous tertiary amine solvents. *J Chem Inf Model* 2021;61(4):1814–24.
- [33] Caplow M. Kinetics of carbamate formation and breakdown. *J Am Chem Soc* 1968;90(24):6795–803.
- [34] Crooks JE, Donnellan JP. Kinetics and mechanism of the reaction between carbon-dioxide and amines in aqueous-solution. *J Chem Soc-Perkin Trans 2* 1989;4:331–3.
- [35] Donaldson TL, Nguyen YN. Carbon dioxide reaction kinetics and transport in aqueous amine membranes. *Ind Eng Chem Fundam* 1980;19(3):260–6.
- [36] Yamada H, et al. Density functional theory study on carbon dioxide absorption into aqueous solutions of 2-amino-2-methyl-1-propanol using a continuum solvation model. *Chem A Eur J* 2011;115(14):3079–86.
- [37] Xie HB, et al. Reaction mechanism of monoethanolamine with CO<sub>2</sub> in aqueous solution from molecular modeling. *J Phys Chem A* 2010;114(43):11844–52.

- [38] Marenich AV, Cramer CJ, Truhlar DG. Universal solvation model based on solute electron density and on a continuum model of the solvent defined by the bulk dielectric constant and atomic surface tensions. *J Phys Chem B* 2009;113(18):6378–96.
- [39] Gaussian 09W Rev. D.01 [computer program]. Wallingford, CT: Gaussian, Inc., 2016.
- [40] Wang K, Shan X, Chen X. Electron propagator theory study of 2-aminoethanol conformers. *J Mol Struct (Thoechem)* 2009;909(1):91–5.
- [41] O'Boyle NM, et al. Open Babel: an open chemical toolbox. *J Cheminform* 2011;3.
- [42] Lu T. Molclus program, Version 1.9.9.7. <http://www.keinsci.com/research/molclus.html>, 2021.
- [43] Stewart JJP. MOPAC: a semiempirical molecular orbital program. *J Comput Aided Mol Des* 1990;4(1):1–103.
- [44] Ma'mun S, Dindore VY, Svendsen HF. Kinetics of the reaction of carbon dioxide with aqueous solutions of 2-((2-aminoethyl)amino)ethanol. *Ind Eng Chem Res* 2007;46(2):385–94.
- [45] Zhong N, et al. Reaction kinetics of carbon dioxide (CO<sub>2</sub>) with diethylenetriamine and 1-amino-2-propanol in nonaqueous solvents using stopped-flow technique. *Ind Eng Chem Res* 2016;55(27):7307–17.
- [46] Hartono A, da Silva EF, Svendsen HF. Kinetics of carbon dioxide absorption in aqueous solution of diethylenetriamine (DETA). *Chem Eng Sci* 2009;64(14):3205–13.
- [47] Sada E, et al. Chemical-kinetics of the reaction of carbon-dioxide with ethanolamines in nonaqueous solvents. *AIChE J* 1985;31(8):1297–303.
- [48] Henni A, Li J, Tontiwachwuthikul P. Reaction kinetics of CO<sub>2</sub> in aqueous 1-amino-2-propanol, 3-amino-1-propanol, and dimethylmonoethanolamine solutions in the temperature range of 298–313k using the stopped-flow technique. *Ind Eng Chem Res* 2008;47(7):2213–20.
- [49] Jamal A, Meisen A, Jim Lim C. Kinetics of carbon dioxide absorption and desorption in aqueous alkanolamine solutions using a novel hemispherical contactor—II: experimental results and parameter estimation. *Chem Eng Sci* 2006;61(19):6590–603.
- [50] Versteeg GF, Van Dijck LAJ, Van Swaaij WPM. On the kinetics between CO<sub>2</sub> and alkanolamines both in aqueous and non-aqueous solutions. An overview. *Chem Eng Commun* 1996;144(1):113–58.
- [51] Teramoto M, et al. Measurement of rate constant of reaction between carbon dioxide and monoprotonated ethylenediamine by chemical absorption method. *J Chem Eng Jpn* 1997;30(1):176–8.
- [52] Gordesli FP, Alper E. The kinetics of carbon dioxide capture by solutions of piperazine and N-methyl piperazine. *Int J Global Warming* 2011;3(1–2):67–76.
- [53] Rinker EB, Sami SA, Sandall OC. Kinetics and modelling of carbon dioxide absorption into aqueous solutions of N-methyldiethanolamine. *Chem Eng Sci* 1995;50(5):755–68.
- [54] Kadiwala S, Rayer AV, Henni A. Kinetics of carbon dioxide (CO<sub>2</sub>) with ethylenediamine, 3-amino-1-propanol in methanol and ethanol, and with 1-dimethylamino-2-propanol and 3-dimethylamino-1-propanol in water using stopped-flow technique. *Chem Eng J* 2012;179:262–71.
- [55] Singto S, et al. The effect of chemical structure of newly synthesized tertiary amines used for the post combustion capture process on carbon dioxide (CO<sub>2</sub>): kinetics of CO<sub>2</sub> absorption using the stopped-flow apparatus and regeneration, and heat input of CO<sub>2</sub> regeneration. *Energy Proc* 2017;114:852–9.
- [56] Versteeg GF, van Swaaij WPM. On the kinetics between CO<sub>2</sub> and alkanolamines both in aqueous and non-aqueous solutions—II. Tertiary amines. *Chem Eng Sci* 1988;43(3):587–91.
- [57] Lu T, Chen Q. Independent gradient model based on Hirshfeld partition: a new method for visual study of interactions in chemical systems. *J Comput Chem* 2022;43(8):539–55.
- [58] Lu T, Chen F. Atomic dipole moment corrected hirshfeld population method. *J Theor Comput Chem* 2012;11(01):163–83.
- [59] Lu T, Chen F. Multiwfns: a multifunctional wavefunction analyzer. *J Comput Chem* 2012;33(5):580–92.
- [60] Humphrey W, Dalke A, Schulten K. VMD: visual molecular dynamics. *J Mol Graph* 1996;14(1):33–8.
- [61] Jorgensen KR, Cundari TR, Wilson AK. Interaction energies of CO<sub>2</sub>-amine complexes: effects of amine substituents. *Chem A Eur J* 2012;116(42):10403–11.
- [62] Xiao M, et al. A study of structure–activity relationships of commercial tertiary amines for post-combustion CO<sub>2</sub> capture. *Appl Energy* 2016;184:219–29.
- [63] Muchan P, et al. Effect of number of amine groups in aqueous polyamine solution on carbon dioxide (CO<sub>2</sub>) capture activities. *Sep Purif Technol* 2017;184:128–34.
- [64] Liu Q, et al. OptCAMD: an optimization-based framework and tool for molecular and mixture product design. *Comp Chemical Eng* 2019;124:285–301.